Bicarbonate kinetics in humans: identification and validation of a three-compartment model

M. P. SACCOMANI, R. C. BONADONNA, E. CAVEGGION, R. A. DEFRONZO, AND C. COBELLI
Department of Electronics and Informatics, University of Padova, 35131 Padua;
Division of Metabolic Diseases, University of Verona, 37124 Verona, Italy; and
Division of Diabetes, University of Texas Health Science Center, San Antonio, Texas 78284

Saccomani, M. P., R. C. Bonadonna, E. Caveggion, R. A. DeFronzo, and C. Cobelli. Bicarbonate kinetics in humans: identification and validation of a three-compartment model. *Am. J. Physiol.* 269 (*Endocrinol. Metab.* 32): E183–E192, 1995.—A model of bicarbonate kinetics is crucial to a correct interpretation of experiments for measuring oxidation in vivo of carbon-labeled compounds. The aim of this study is to develop a compartmental model of bicarbonate kinetics in humans from tracer data by devoting particular attention to model identification and validation. The data base consisted of impulse-dose studies of ^{14}C-labeled bicarbonate in nine normal subjects. The decay curve of specific activity of CO_2 in expired air ($sa^R_{CO_2}$) was frequently sampled for 4–7 h. In addition, endogenous production of CO_2, $\dot{V}_{CO_2}$, was measured by indirect calorimetry. A model of data, i.e., an exponential model, analysis of decay curves of $sa^R_{CO_2}$ showed first that three compartments are necessary and sufficient to describe bicarbonate tracer kinetics. Compartmental models were then used as models of system. To correctly describe the input-output configuration, labeled CO_2 flux in the expired air, $\Phi^R_{CO_2}$ ($= sa^R_{CO_2} \cdot \dot{V}_{CO_2}$), has been used as measurement variable in tracer model identification. A mammillary three-compartment model with a respiratory and a nonrespiratory loss has been studied. Whereas there is good evidence that respiratory loss takes place in the central compartment, whether nonrespiratory loss is taking place in the central compartment or in one of the two peripheral compartments is uncertain. Thus three competing tracer models were considered. Using a model-independent analysis of data, based on the body activity variable, to calculate mean residence time in the system, we have been able to validate a specific model structure, i.e., with the two irreversible losses taking place in the central compartment. This validated tracer model was then used to quantitate bicarbonate masses in the system. Because there is uncertainty about where endogenous production enters the system, lower and upper bounds of masses of bicarbonate in the body are derived.

tracer kinetics; compartmental model; model identification; model validation; parameter estimation

THE BICARBONATE SYSTEM plays an important role in measuring from tracer data the oxidation of substrates in the human body. In fact, many substrates are metabolized by the oxidation process, producing CO_2, which can be measured in the expired air. This measure depends not only on the metabolism of the individual substrate but also on the kinetics of bicarbonate in the body (4, 10, 13, 15, 19). Thus the knowledge of the distribution and metabolism of bicarbonate is crucial to a correct interpretation of experiments for measuring oxidation in vivo of carbon-labeled compounds. The models of bicarbonate kinetics employed in substrate oxidation tracer studies are linear compartmental models and have been usually identified from an experiment involving an impulsive intravenous input of labeled bicarbonate ([^{14}C]- or [^{13}C]$NaHCO_3$) and frequent sampling of labeled CO_2 in the expired air. However, there is uncertainty concerning the model structure; e.g., three- (1, 11 18, 20) and two-compartment (6, 17, 21) models have been proposed; in addition, different output variables have been considered for model identification, e.g., the specific activity or enrichment of CO_2 (1, 6, 13, 15, 18–20) and the labeled CO_2 flux (4, 10, 11, 17, 21) in the expired air; this in turn has determined the adoption of different model parameterization.

The aim of this study is to develop a compartmental model of bicarbonate kinetics in humans from tracer data by devoting particular attention to aspects related to model identification and validation. Various candidate compartmental structures are tested. The role of the output variable chosen for model identification is explicitly examined. Finally, a model-structure-independent analysis of the data, based on the activity variable (2, 12, 16), is used in the validation process to select the most plausible compartmental structure. From this validated structure, lower and upper bounds of masses of bicarbonate in the body are derived.

EXPERIMENT, MEASUREMENTS, AND DATA BASE

Nine healthy volunteers were studied. All were within 20% of desirable body weight (Metropolitan Life Insurance Tables, 1983), had systolic and diastolic blood pressures within normal limits, and had no family history of diabetes mellitus. No subjects had clinical or laboratory evidence of heart, liver, and kidney disease, as ascertained by the collection of medical history, a complete physical examination, and laboratory blood and urine testing. All subjects had normal glucose tolerance according to the National Diabetes Data Group criteria. All subjects consumed an isocaloric diet containing >200 g of carbohydrates per day for ≥ 3 days before the study. The purpose, nature, and potential risks of

the study were explained to all subjects, and informed written consent was obtained before their participation. The protocol was reviewed and approved by the Human Investigation Committees at the Yale University School of Medicine and the University of Texas Health Science Center at San Antonio.

An impulse dose of radiolabeled bicarbonate ([^{14}C]$NaHCO_3$) was intravenously administered to each subject. All studies were performed at 8:30 A.M. after an overnight (10- to 12-h) fast. In all subjects, a 20-gauge Teflon catheter was inserted into an antecubital vein and kept patent with intermittent flushes of normal saline. Twenty microcuries of $NaH^{14}CO_3$ (New England Nuclear, Boston, MA) were brought to a volume of 20 ml with sterile normal saline and divided into two aliquots. The first ($\simeq$16 ml) aliquot was injected through the venous catheter in $<$10 s at *time 0*. The catheter was immediately flushed with 10 ml of sterile saline. The volume of tracer injected was determined gravimetrically. The second aliquot ($\simeq$4 ml) was dispensed in a preweighed tube containing 200 ml of 4 N NaOH. The tube was weighed again to determine the exact amount of tracer added to it and stored at −20°C until the end of the study. The decay curve of specific activity of CO_2 in the expired air ($sa^R_{CO_2}$, dpm/mmol) was frequently sampled for 4–7 h. In five subjects, samples were taken at 1, 2, 3, 4, 5, 7, 9, 11, 13, 15, 18, 21, 24, 27, 30, 35, 40, 45, 50, 55, 60, 70, 80, 90, 100, 120, 140, 160, 180, 200, 220, 240, 260, 300, 340, 380, and 420 min, and in four subjects, samples were only taken until 240 min. Figure 1 shows the specific activity data of all studies.

Samples for the determination of CO_2 specific activity were collected and treated as follows. At predetermined time points, subjects were asked to blow through a flexible plastic conduit (40 cm long, 4 mm diam), equipped with a one-way valve, into plastic tubes containing variable amounts of an ice-cold CO_2-trapping solution (1 M hyamine hydroxide in methanol/absolute ethanol/0.1% phenolphthalein in absolute ethanol in volume ratios of 3:5:1, respectively). For each sample, the collection of expired air was stopped when the indicator of the trapping solution turned from pink to colorless.

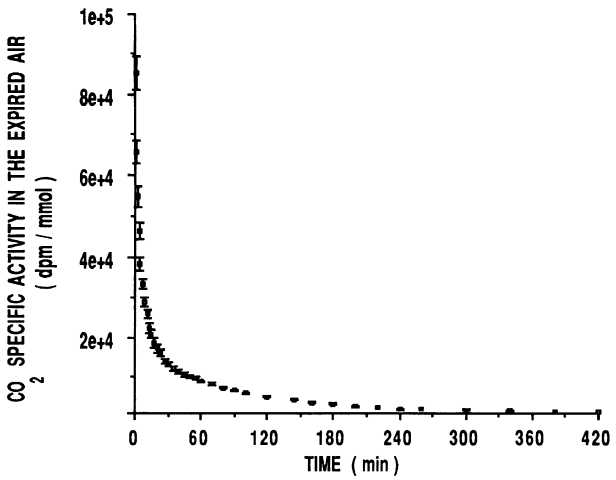

Fig. 1. CO_2 specific activity (means ± SE) in expired air, $sa^R_{CO_2}$.

The exact amount of acid trapped at the turning point of phenolphthalein was determined by addition of known amounts of 1 N HCl to 3 ml of the trapping solution. This titration factor was checked weekly for each batch of the trapping solution. The tubes were capped and kept in melting ice until the end of the study. The expired air collected from 1 to 24 min, from 27 to 55 min, and from 60 min to the end of the study was bubbled through 500 μl and 1 and 3 ml of trapping solution, respectively. A sample of expired air was also collected before tracer injection into 3 ml of trapping solution (blank sample). Samples were kept in ice until the end of the study and then immediately processed. Duplicate aliquots (200 μl from 1 to 24 min, 400 μl from 27 to 55 min, and 1 ml from 60 min to the end of the study) of the samples were pipetted into scintillation vials, mixed with scintillation fluid (Scinti-Verse II, Fisher Scientific), and counted in a Tri-Carb scintillation β-counter (Packard Instruments, Downers Grove, IL), with external standard correction for quenching. At each time point, radioactivity was averaged and CO_2 specific activity, after subtraction of blank activity, was calculated as follows: $sa^R_{CO_2}$ (dpm/mmol) = [sample dpm/sample volume (ml)] × 3.

Computerized open-circuit indirect calorimetry (Vista, Vacumed, Ventura, CA) was used to measure the excretion rate of CO_2. A transparent ventilated hood was placed over the subject's head and made airtight around the neck. A slight negative pressure was maintained in the hood to avoid loss of expired air. Ventilation was measured by means of a dry gas meter. A constant fraction of the air flowing out of the hood was automatically collected for gas analysis. CO_2 was measured by an infrared analyzer with use of an Applied Electrochemistry instrument (Sunnyvale, CA).

MODELS OF DATA

Before a model of system is built, a model of data is useful to determine the model order, i.e., the number of compartments that is necessary and sufficient to describe the data. Because the dynamics of a tracer in a steady-state system are linear and time invariant (3), an exponential model of the data is theoretically correct to describe the $sa^R_{CO_2}$ data.

In particular, three models characterized by two, three, and four exponentials, respectively, were fitted to the tracer data of each experiment as follows

$$y(t) = A_1 e^{-\alpha_1 t} + A_2 e^{-\alpha_2 t} \quad (1)$$

$$y(t) = A_1 e^{-\alpha_1 t} + A_2 e^{-\alpha_2 t} + A_3 e^{-\alpha_3 t} \quad (2)$$

$$y(t) = A_1 e^{-\alpha_1 t} + A_2 e^{-\alpha_2 t} + A_3 e^{-\alpha_3 t} + A_4 e^{-\alpha_4 t} \quad (3)$$

Thus discrete time measurements, $z(t_l) = sa^R_{CO_2}(t_l)$, where t_l denotes the sampling time of the lth measurement ($l = 1, 2, \ldots, N$), and model predictions, $y(t_l)$, are related by

$$z(t_l) = sa^R_{CO_2}(t_l) = y(t_l) + e(t_l) \quad (4)$$

where $e(t_l)$ is the measurement error at t_l. The measure-

ment error was assumed additive, uncorrelated with zero mean, and Gaussian with an experimentally derived variance.

In particular, the postulated model for the error variance was

$$\sigma^2(t_l) = a^2 + b^2[z(t_l)]^c \quad (5)$$

where a, b, and c are constant parameters. The values of a, b, and c have been estimated using extended least squares (14). Typical values were $a = 30$, $b = 0.035$, and $c = 2$, and thus measurement errors ranged from a coefficient of variation $[\sigma(t_l)/z(t_l)]$ of 3% at high counts to 12% at low counts.

The exponential model parameters were estimated using nonlinear least squares with optimally chosen weights; i.e., each datum was weighted inversely proportional to its measurement variance (3). The selection of the best exponential model was made on the basis of criteria such as *1*) pattern of normalized residual errors, i.e., the difference between data and model predictions weighted inversely to the data standard deviations (3), *2*) precision of parameter estimates evaluated from the inverse of the Fisher information matrix **J** (3), and *3*) parsimony criteria, e.g., the Akaike and the Schwarz criteria (3), which take into account goodness of fit and parameter number.

Only the parameters of the two- and three-exponential models were estimated with good precision: the coefficient of variation of parameter estimates was usually well below 20%. The three-exponential model was definitely superior to the two-exponential model, in terms of normalized residual errors (Fig. 2) and the parsimony criteria of Akaike and Schwarz (Table 1). The parameter estimates of the three-exponential model are shown in Table 2. No difference in parameter values was observed between subjects monitored for 4 and 7 h.

COMPARTMENTAL MODELS AS MODELS OF SYSTEM

Linear time-invariant compartmental models were proposed as models of system of the tracer data. Given

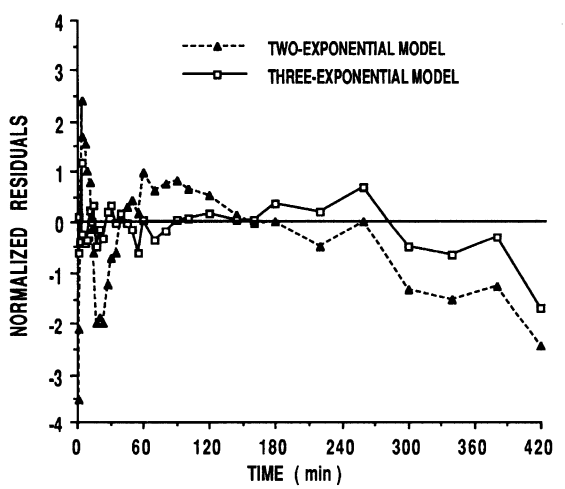

Fig. 2. Normalized residual errors (mean) of two- and three-exponential models of CO_2 specific activity in expired air.

Table 1. *Results of parsimony criteria of Akaike and Schwarz*

Subj No.	Model			
	Two exponential		Three exponential	
	AIC	SC	AIC	SC
1	193.09	199.31	69.64	78.97
2	211.48	217.59	36.22	45.38
3	91.17	97.39	39.61	48.94
4	78.66	84.65	28.44	37.42
5	140.22	145.40	101.58	109.36
6	40.77	46.24	21.37	29.57
7	85.17	90.77	54.65	63.06
8	39.63	45.23	28.11	36.52
9	64.83	70.43	27.46	35.87

AIC, criteria of Akaike; SC, criteria of Schwarz.

the superiority of the three-exponential model in fitting the data and in line with previously published models, we assumed a mammillary structure with the accessible compartment exchanging with two peripheral compartments. The model is given by

$$\dot{\mathbf{q}}(t) = \mathbf{A}\mathbf{q}(t) + \mathbf{u}(t) \quad (6)$$

where $\mathbf{q}$ denotes the derivative of $\mathbf{q}$ with respect to time, $\mathbf{q} = [q_1\ q_2\ q_3]^T$ is the state vector of bicarbonate tracer quantities in the three compartments, $\mathbf{u} = [u_1\ 0\ 0]^T$ is the test tracer input vector; and $\mathbf{A}$ is a 3×3 matrix, the elements of which are related to the unknown transfer rate constants k_{ij} of the model as follows

$$a_{ij} = k_{ij} \geq 0, \quad i,j = 1, 2, 3, \quad i \neq j \quad (7)$$

$$a_{ii} = -\sum_{\substack{j=0 \\ j \neq i}}^{3} k_{ji}, \quad k_{0i} \geq 0 \quad (8)$$

Table 2. *Three-exponential model parameters*

Subj No.	A_1	A_2	A_3	α_1	α_2	α_3
1	66,430 (9)	35,420 (8)	12,950 (3)	0.457 (13)	0.073 (6)	0.008 (1)
2	87,830 (7)	26,090 (8)	14,690 (3)	0.477 (9)	0.067 (8)	0.009 (1)
3	45,260 (11)	34,290 (12)	17,160 (2)	0.371 (20)	0.075 (9)	0.009 (1)
4	77,310 (11)	27,080 (21)	13,150 (2)	0.386 (17)	0.094 (13)	0.009 (1)
5	68,400 (6)	8,647 (13)	12,490 (10)	0.241 (8)	0.028 (24)	0.009 (4)
6	47,750 (32)	24,950 (17)	14,230 (2)	0.599 (32)	0.113 (12)	0.011 (2)
7	61,890 (21)	35,100 (15)	14,610 (2)	0.485 (25)	0.102 (10)	0.010 (2)
8	40,790 (8)	7,758 (25)	15,230 (11)	0.195 (15)	0.037 (43)	0.011 (5)
9	56,690 (8)	16,630 (19)	17,000 (6)	0.273 (15)	0.054 (20)	0.011 (3)
Mean	61,372	23,996	14,612	0.387	0.071	0.0097
±SD	±15,492	±10,771	±1,663	±0.132	±0.029	±0.001
Mean CV ($\hat{p}_i$)	(12)	(15)	(5)	(17)	(16)	(2)

A_1, A_2, and A_3 are expressed in dpm/mmol; α_1, α_2, and α_3 are expressed in min^{-1}. Values in parentheses represent precision of parameter estimate ($\hat{p}_i$) expressed as $CV(\hat{p}_i) = SD(\hat{p}_i)/\hat{p}_i \times 100$, where CV is coefficient of variation.

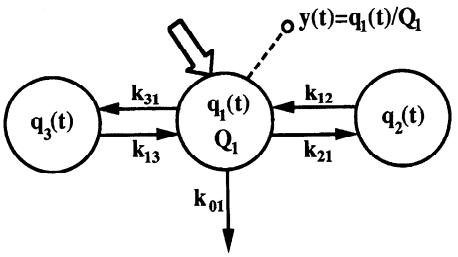

Fig. 3. Three-compartment model with specific activity as output and one irreversible loss from central compartment.

Physiological information must guide the selection of the structure of **A**. Whereas no uncertainty exists on the presence of k_{21}, k_{12}, k_{31}, and k_{13}, i.e., the transfer rate constants describing exchange between the accessible and the two peripheral compartments (*pool 2* is assumed to be rapidly exchanging while *pool 3* is slowly exchanging), the selection of the sites of irreversible loss of bicarbonate, i.e., the nonzero k_{01},k_{02},k_{03} is more problematic. Different model parameterizations have been proposed in the literature, depending on the output variable, i.e., CO_2 specific activity or enrichment and labeled CO_2 flux in the expired air, which are chosen for their identification (see below).

Modeling was based on methodology described previously (3). Salient ingredients included a priori identifiability analysis, nonlinear least-squares parameter estimation, and assessment of identification results by evaluation of normalized residual errors and evaluation of precision of parameter estimates (from the inverse of the Fisher information matrix).

From the tracer model, other kinetic parameters can be calculated. Of particular interest is the mean total residence time in the system (6) of a particle entering, e.g., *pool 1*, which is given by

$$\mathrm{MRT}_1 = \sum_{i=1}^{3} \theta_{i1} \qquad (9)$$

where θ_{ij} is the generic element of the mean residence time matrix

$$\Theta = -\mathbf{A}^{-1} \qquad (10)$$

Once the tracer model structure has been fixed, the specification of the site(s) of entry of endogenous bicarbonate production(s) defines the steady-state tracee model, which has as unknown the pool sizes (Q_i) and the production(s) (P).

SPECIFIC ACTIVITY AS OUTPUT VARIABLE IN TRACER MODEL IDENTIFICATION

First we tested the three-compartment mammillary model employed previously (13, 15, 18–20), which has one irreversible loss only from the central compartment (Fig. 3) and has been identified using specific activity in the expired air as measurement variable. The accessible central compartment represents CO_2 in the pulmonary circulation, which equilibrates very rapidly with the expired air, whereas the peripheral *pools 2* and *3* are tissues in slow and fast equilibration, respectively, with the central compartment. Thus labeled bicarbonate entering the accessible compartment can exchange with one of the two peripheral compartments and/or can leave the system through the irreversible loss taking place in the accessible central compartment. The model state equation is *Eq. 6*. The model output, i.e., specific activity in the expired air, is as follows

$$y(t) = \frac{q_1(t)}{Q_1} \qquad (11)$$

where Q_1 is the unknown bicarbonate mass of the accessible compartment.

The measurement equation (cf. *Eq. 4*) is as follows

$$z(t_l) = sa^{R}_{CO_2}(t_l) = y(t_l) + e(t_l) = \frac{q_1(t)}{Q_1} + e(t_l) \qquad (12)$$

The unknown parameters of the model are the rate constants k_{ij} and Q_1, and they are a priori uniquely identifiable. Model fit (Fig. 2) and precision of parameter estimates (not shown) were very good in all cases.

However, a problem arises with this model as far as description of measurement is concerned. The specific activity data are assumed to be taken from *pool 1*, which is also the pool where the tracer input of bicarbonate takes place. Thus the model assumes that the whole dose distributes in the volume of the sampled compartment. However, the specific activity is measured in a pool that is in equilibrium with *pool 1* but in which only a fraction of the dose is present.

This model has been often used to estimate the endogenous CO_2 production (P), which is assumed to take place in *pool 1* (the following also holds if P enters *pool 2* or *3*). By solving the steady-state tracee equations (3 equations in 3 unknowns Q_2, Q_3, and P, because Q_1 is known from the tracer model), one can estimate P (Table 3). The endogenous production of CO_2 can also be measured in a model-independent fashion by indirect calorimetry, and thus one can compare the model esti-

Table 3. *Comparison between model-derived estimate of bicarbonate production and indirect calorimetry measurement*

Parameters	Subj No. 1	2	3	4	5	6	7	8	9	Mean	±SD
P	10.08	15.63	13.61	15.18	14.42	9.52	10.27	10.93	10.10	12.19	±2.47
$\dot{V}CO_2$	9.00	13.16	11.17	12.50	10.93	7.63	9.38	7.79	8.37	9.99	±2.03

Values are expressed in mmol/min. P, model-derived estimate of bicarbonate production; $\dot{V}CO_2$, indirect calorimetry measurement of endogenous CO_2 production.

mate P with the independent indirect calorimetry $\dot{V}_{CO_2}$ measurement. As shown in Table 3, the model systematically overestimates $\dot{V}_{CO_2}$. This result can be justified by thinking that the irreversible loss k_{01} is accounting for the respiratory and nonrespiratory losses (e.g., bone, urine, sweat) of the tracer, because the recycling of the tracer lost through the nonrespiratory pathway does not occur in any appreciable extent during the time horizon of the study. In fact, typical values for the recovery in the expired air of the injected tracer dose in basal kinetic studies have been found to range from 50 to 90% (cf. review in Ref. 9; 1, 4, 11, 20, 21). However, for the tracee, the nonrespiratory loss is not an irreversible pathway; thus an additional very slow pool must be envisioned at the end of the nonrespiratory loss, which is continuously feeding back the accessible pool with a CO_2 flux. Thus the tracee model based on the tracer model of Fig. 3, which assumes both losses to be irreversible, overestimates the endogenous production of CO_2.

USE OF $\dot{V}_{CO_2}$ INFORMATION IN TRACER MODEL IDENTIFICATION

To overcome the problem of the model of Fig. 3 in correctly describing the input-output experiment, one can take advantage of the additional information from the $\dot{V}_{CO_2}$ measurement. The incorporation into the system-experiment model of the specific activity and $\dot{V}_{CO_2}$ measurements can be done, however, in different ways.

Recovery factor constraint and specific activity as output variable. A first attempt consists of calculating the recovered dose (D^R), i.e., the portion of the injected dose (D) recovered and sampled in the expired air. This allows us to remove the structural error present in the model of Fig. 3. In fact, by considering D^R as the input dose, the irreversible loss k_{01} is now responsible only for the respiratory pathway. To do this, one has to multiply all the points of the specific activity decay curve by the $\dot{V}_{CO_2}$ value, thus obtaining the time course of the flux of labeled CO_2 eliminated from the respiratory system($\phi^R_{CO_2}$, dpm/min). Now the recovered dose is given by

$$D^R = \int_0^\infty \phi^R_{CO_2}(t)\,dt = \int_0^\infty \dot{V}_{CO_2}\, sa^R_{CO_2}(t)\,dt = \dot{V}_{CO_2}\left(\frac{A_1}{\alpha_1}+\frac{A_2}{\alpha_2}+\frac{A_3}{\alpha_3}\right) = \frac{A'_1}{\alpha_1}+\frac{A'_2}{\alpha_2}+\frac{A'_3}{\alpha_3} \quad (13)$$

where A_i and α_i (i = 1, 2, 3) are the parameters of the exponential model describing specific activity (cf. *Eq. 3*) and $A'_i = \dot{V}_{CO_2} \cdot A_i$ (i = 1, 2, 3).

In this way, the error of the model of Fig. 3 is removed. One can now identify the model of Fig. 3 from the specific activity measurement, and it is easy to anticipate that one will recover the correct value of the endogenous production of CO_2. However, this approach will tell nothing about the nonrespiratory pathway. In addition, the goal here is to arrive at a bicarbonate model usable in substrate oxidation studies, and *Eq. 13* may become difficult to apply. In fact, because the label is introduced into the substrate, $sa^R_{CO_2}$ is expected to rise from zero and subsequently decrease after termination of the label administration; there is thus the need to monitor $sa^R_{CO_2}$ for long enough after termination of the label administration to perform the integral operation of *Eq. 13*. Thus there is the need to describe the respiratory and nonrespiratory losses, and one must envision other ways to use the additional $\dot{V}_{CO_2}$ measurement information.

An approach has been recently proposed in the modeling study by Barstow et al. (1). They have used the recovery factor calculated as

$$Rec = \frac{D^R}{D} \quad (14)$$

where D^R is given by *Eq. 13* as a constraint in their model of Fig. 4, *top*, to distinguish between the respiratory and nonrespiratory losses

$$Rec = \frac{\int_0^\infty k^R_{01} q_1(t)\,dt}{\int_0^\infty k^R_{01} q_1(t)\,dt + \int_0^\infty k^{NR}_{01} q_1(t)\,dt} = \frac{k^R_{01}}{k^R_{01}+k^{NR}_{01}} \quad (15)$$

where the superscripts R and NR refer to the respiratory and nonrespiratory pathways, respectively.

However, because the recovery factor constraint is imposed on the model identified from specific activity data, the structural error of considering the output measurement in the expired air being in the same compartment where the whole dose distributes remains.

An additional limitation of the recovery factor constraint approach is that it only allows consideration of the two irreversible losses as both taking place in

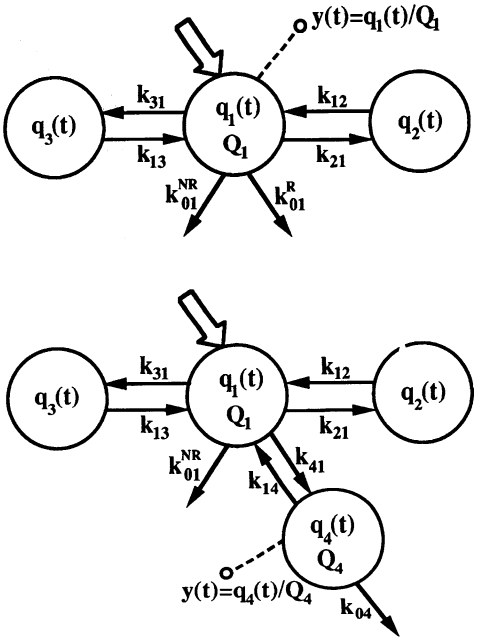

Fig. 4. *Top*: three-compartment model, with specific activity as output, describing explicitly respiratory and nonrespiratory losses. *Bottom*: correct model to describe specific activity data.

compartment 1. Whereas there is good evidence that the respiratory loss is taking place in the accessible compartment, there is uncertainty about where the nonrespiratory loss is taking place. However, only if both irreversible losses take place in *compartment 1*, the recovery factor can be used to provide the independent relation between k_{01}^{R} and k_{01}^{NR} given by *Eq. 15*; e.g., if the nonrespiratory loss takes place in *compartment 2*, the recovery factor would also be a function of the unknown term $\int_0^\infty q_2(t)dt$. Finally, the only way to correctly identify the model of Fig. 4, *top*, from specific activity data would be to separate the input from the output compartment. Thus the model should have the structure depicted in Fig. 4, *bottom*, where k_{01} corresponds to the k_{01}^{NR} of the model of Fig. 4, *top*; *compartment 4* is the sampled compartment and represents CO_2 in the expired air, which is in equilibrium with *compartment 1*, where the input dose enters, and k_{04} represents the respiratory loss. However, this model is not identifiable from the specific activity data.

$\phi^R_{CO_2}$ as output variable. By use of $\phi^{R}_{CO_2}$ as the measurement variable for model identification, the error in describing the input-output experiment of the model of Fig. 4, *top*, vanishes.

The new system-experiment model is shown in Fig. 5, *model I*. In addition, the use of $\phi^{R}_{CO_2}$ allows us to test the alternative plausible compartmental structures with the nonrespiratory loss in *compartment 2* or *3* (Fig. 5, *models II* and *III*).

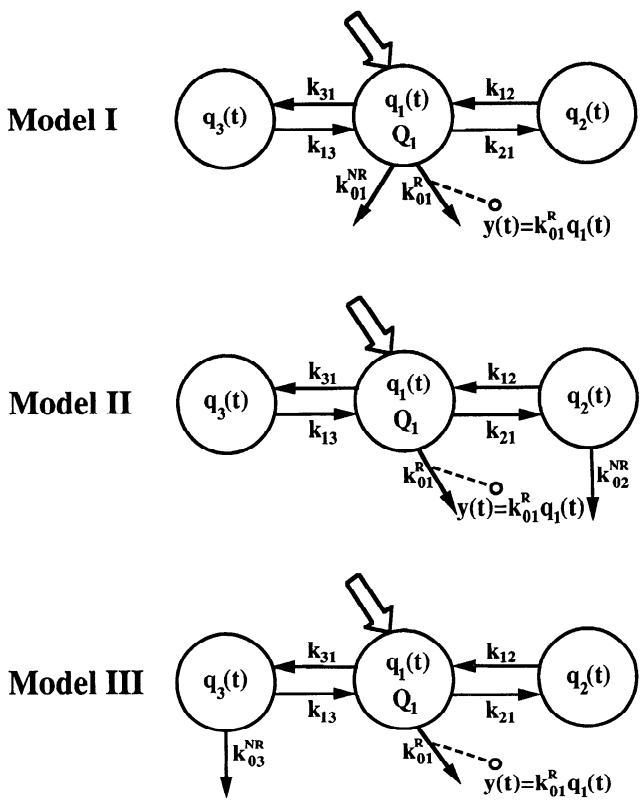

Fig. 5. Three models with labeled CO_2 flux as output. *Models I–III* differ in site of nonrespiratory loss.

The state equation of each model is *Eq. 6*. The model output and measurement equations are the same for all three models

$$y(t) = k_{01}^{R} q_1(t) \tag{16}$$

$$z(t_l) = \phi^{R}_{CO_2}(t_l) = y(t_l) + e(t_l) = k_{01}^{R} q_1(t_l) + e(t_l) \tag{17}$$

Now $e(t_l)$ has to account for the error arising from the specific activity measurement as well as for the error arising from the $\dot{V}_{CO_2}$ measurement. In particular, this second error accounts for the error of the instrument, which is negligible ($\sim 1\%$), and that caused by the fact that the $\dot{V}_{CO_2}$ value is the average value ($\sim 7\%$). If the two error components are assumed to be independent, $e(t_l)$ ranges, in terms of coefficient of variation, from 7 to 14%.

All three models can be shown to be a priori uniquely identifiable. The parameters of all three models were estimated with good precision, and the model fit was equally good for all three models. The parameter estimates and their precision in the three models are shown in Table 4, and a representative fit of *model I* is shown in Fig. 6.

VALIDATION OF THE TRACER COMPARTMENTAL MODELS

Having arrived at three physiologically plausible compartmental structures, it is important to resort to model-structure-independent approaches to validate them. By comparing some structure-dependent parameter estimates with the corresponding estimates calculated by structure-independent approaches, it may be possible to reject some compartmental structures. We discuss below a model-independent approach to calculate the mean residence time in the system and show its role in the validation stage of the tracer model structures.

Mean residence time. The mean residence time parameter can be calculated in a model-independent fashion by use of the "body activity" variable [BA(t)], i.e., the amount of tracer in the system at *time t* (2, 12, 16)

$$\mathrm{MRT_{BA}} = \frac{\int_0^\infty \mathrm{BA}(t)\, dt}{D} \tag{18}$$

For the bicarbonate system, because the only irreversible losses are k_{01}^{R} and k_{0i}^{NR} with i = 1, 2 or 3 depending on the particular model chosen, the numerator of *Eq. 18* can be calculated as follows

$$\int_0^\infty \mathrm{BA}(t)\, dt = \int_0^\infty \left[D - \int_0^t \phi^{R}_{CO_2}(s)\, ds - \int_0^t \phi^{NR}_{CO_2}(s)\, ds \right] dt \tag{19}$$

However, the flux $\phi^{NR}_{CO_2}$ cannot be evaluated from the data, and we are only able to calculate the mean residence time of a particle belonging to the dose fraction D^R, which will leave the system by the respira-

Table 4. *Parameter estimates and their precision in compartmental models I–III*

Subj No.	*Model I*						*Model II*						*Model III*					
	k_{21}	k_{12}	k_{31}	k_{13}	k_{01}^{R}	k_{01}^{NR}	k_{21}	k_{12}	k_{31}	k_{13}	k_{01}^{R}	k_{02}^{NR}	k_{21}	k_{12}	k_{31}	k_{13}	k_{01}^{R}	k_{03}^{NR}
1	0.166	0.221	0.067	0.023	0.046	0.005	0.172	0.214	0.067	0.023	0.046	0.007	0.166	0.221	0.072	0.021	0.046	0.002
	(56)	(39)	(25)	(11)	(18)	(21)	(55)	(40)	(25)	(11)	(18)	(30)	(56)	(39)	(24)	(12)	(18)	(17)
2	0.206	0.181	0.070	0.026	0.051	0.009	0.215	0.173	0.070	0.026	0.051	0.008	0.206	0.181	0.079	0.023	0.051	0.003
	(26)	(22)	(22)	(10)	(12)	(12)	(26)	(22)	(22)	(10)	(12)	(17)	(26)	(22)	(20)	(12)	(12)	(10)
3	0.106	0.217	0.054	0.028	0.032	0.007	0.113	0.203	0.054	0.028	0.032	0.013	0.106	0.217	0.061	0.025	0.032	0.003
	(48)	(40)	(19)	(9)	(10)	(11)	(46)	(42)	(19)	(9)	(10)	(24)	(48)	(40)	(18)	(10)	(10)	(7)
4	0.109	0.171	0.098	0.029	0.051	0.011	0.120	0.156	0.098	0.029	0.051	0.016	0.109	0.171	0.098	0.026	0.051	0.003
	(48)	(41)	(26)	(9)	(19)	(14)	(45)	(44)	(26)	(9)	(19)	(30)	(48)	(41)	(24)	(10)	(19)	(11)
5	0.120	0.075	0.025	0.021	0.035	0.011	0.131	0.068	0.025	0.021	0.035	0.006	0.120	0.075	0.036	0.015	0.035	0.007
	(21)	(27)	(93)	(37)	(11)	(10)	(20)	(27)	(93)	(37)	(11)	(37)	(21)	(28)	(66)	(63)	(11)	(26)
6	0.204	0.318	0.104	0.043	0.045	0.011	0.216	0.302	0.104	0.043	0.045	0.017	0.204	0.318	0.115	0.039	0.045	0.004
	(112)	(55)	(54)	(12)	(45)	(36)	(108)	(58)	(54)	(12)	(45)	(43)	(112)	(55)	(52)	(14)	(45)	(16)
7	0.153	0.266	0.095	0.033	0.054	0.005	0.157	0.257	0.095	0.033	0.053	0.009	0.153	0.266	0.100	0.031	0.054	0.002
	(88)	(48)	(35)	(9)	(31)	(21)	(85)	(50)	(35)	(9)	(31)	(45)	(88)	(48)	(34)	(10)	(31)	(24)
8	0.078	0.086	0.019	0.027	0.025	0.010	0.088	0.076	0.019	0.027	0.025	0.010	0.078	0.086	0.029	0.018	0.025	0.009
	(37)	(54)	(168)	(71)	(15)	(13)	(33)	(53)	(168)	(71)	(14)	(71)	(37)	(54)	(115)	(125)	(15)	(40)
9	0.101	0.123	0.038	0.029	0.036	0.007	0.108	0.115	0.038	0.029	0.036	0.008	0.101	0.123	0.046	0.024	0.036	0.005
	(37)	(43)	(59)	(29)	(14)	(13)	(35)	(44)	(59)	(28)	(14)	(42)	(37)	(43)	(51)	(37)	(14)	(20)
Mean	0.138	0.184	0.063	0.029	0.042	0.008	0.147	0.174	0.063	0.029	0.042	0.010	0.138	0.184	0.071	0.025	0.042	0.004
±SD	±0.046	±0.081	±0.032	±0.006	±0.010	±0.002	±0.046	±0.079	±0.032	±0.006	±0.010	±0.004	±0.046	±0.081	±0.030	±0.007	±0.010	±0.002

Values are expressed in min^{-1}. Values in parentheses represent precision of parameter estimate $\hat{p}_i$ expressed as $CV(\hat{p}_i) = SD(\hat{p}_i)/\hat{p}_i \times 100$.

tory pathway (MRT_{BA}^{R})

$$MRT_{BA}^{R} = \frac{\int_0^{\infty}\left[D^{R} - \int_0^{t} \phi_{CO_2}^{R}(s)\,ds\right]dt}{D^{R}} = \frac{A_1'/\alpha_1^2 + A_2'/\alpha_2^2 + A_3'/\alpha_3^2}{A_1'/\alpha_1 + A_2'/\alpha_2 + A_3'/\alpha_3} \quad (20)$$

where A_i' and α_i ($i = 1, 2, 3$) have been defined in *Eq. 13*. MRT_{BA}^{R} has been calculated for each individual subject (Table 5).

To compare these model-independent body activity results with those obtainable with the three tracer models of Fig. 5, one has to define the analogue of MRT_{BA}^{R} in a compartmental setting, MRT^{R}. To do this, we used the formula proposed by Hearon (8), which gives the mean residence time of those particles that exit irreversibly from the system, the ith compartment, irrespective of their initial location, θ_i

$$\theta_i = \mathbf{u}_i^{T}\Theta^2\mathbf{x}_0/\mathbf{u}_i^{T}\Theta\mathbf{x}_0 \quad (21)$$

where Θ is defined in *Eq. 10*, $\mathbf{u}_i^{T} = [0, 0, \ldots, 1, \ldots, 0]$ is a vector with 1 in the ith position and 0 elsewhere, and $\mathbf{x}_0$ is the initial condition vector. We can thus calculate MRT^{R} as θ_1. The results are shown in Table 5 together with the corresponding results obtained with the model-independent approach (*Eq. 20*). By comparing them, it is clear that the model that better approximates the results obtained with the model-independent approach is *model I*, the model with the nonrespiratory loss taking place in the central accessible compartment; in particular, it provides the same results. Thus *model I* is the model of choice. *Model I* also allows the calculation of the recovery factor, shown in Table 6, by use of *Eq. 15*.

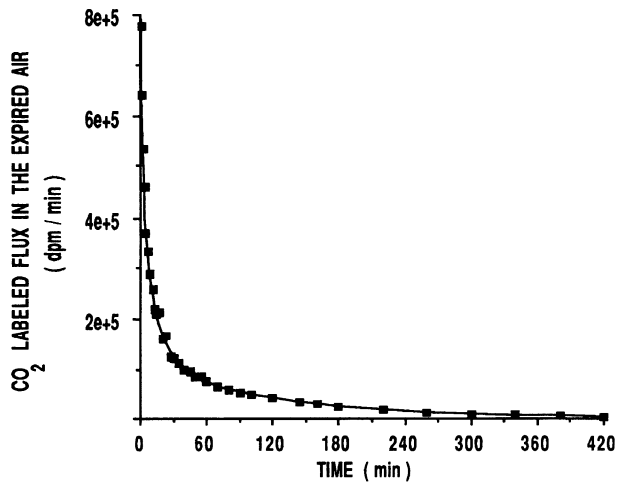

Fig. 6. *Model I* fit (continuous line) of CO_2 labeled flux data in expired air, $\phi_{CO_2}^{R}$, in a representative study (*subj.* 1).

THE TRACEE MODEL

With the model structure fixed for the tracer, it is now possible to turn to the tracee model. Its definition

Table 5. *Mean residence time*

Subj No.	MRT_{BA}^{R}	MRT^{R} *Model I* ($k_{01}^{NR} \neq 0$)	MRT^{R} *Model II* ($k_{02}^{NR} \neq 0$)	MRT^{R} *Model III* ($k_{03}^{NR} \neq 0$)
1	91.23	91.23	90.71	88.20
2	79.10	79.10	79.79	80.28
3	85.81	85.81	88.15	89.10
4	79.27	79.27	80.63	76.34
5	81.73	81.73	83.67	79.99
6	71.12	71.12	71.84	73.02
7	75.95	75.95	76.30	73.62
8	76.00	76.01	74.02	75.66
9	72.57	72.57	72.78	71.34
Mean	79.20	79.20	79.77	78.62
±SD	±6.37	±6.37	±6.73	±6.42

Values are expressed in min.

Table 6. *Recovery factor calculated from model I*

Subj No.	Recovery Factor
1	0.89
2	0.84
3	0.82
4	0.82
5	0.75
6	0.80
7	0.91
8	0.71
9	0.83
Mean ± SD	0.82 ± 0.06

requires specification of the exact site(s) of entry of endogenous production of CO_2 (P) into the system. However, a priori knowledge of the exact site(s) of entry of CO_2 is lacking, and we have thus taken, following Barstow et al. (1), a parameter-bound approach for quantifying three tracee systems. Three tracee models were considered characterized by entry of the endogenous CO_2 production in *compartments 1*, *2*, and *3*, respectively (Fig. 7). Each consists of four compartments, the fourth of which was representative of those tissues where the bicarbonate is fixed very slowly (e.g., bone, urine, sweat) and was not "seen" by the tracer; i.e., k_{41}, in the models of Fig. 7 equals k_{01}^{NR} in the models of Fig. 5. We have neglected, for physiological reasons, the possibility that CO_2 endogenous production can enter *pool 4*. The uncertainty concerning the site of entry of P has no consequences in the estimate of P itself because of the structure of the tracee models; i.e., each of the three models gives the same value of P, which is identical to the value of the $\dot{V}_{CO_2}$ measurement. The situation is different for the pool sizes and thus for the total CO_2 mass in the system. First, the mass of *compartment 1*, Q_1, is not affected by the uncertainty in the site of entry of P, because

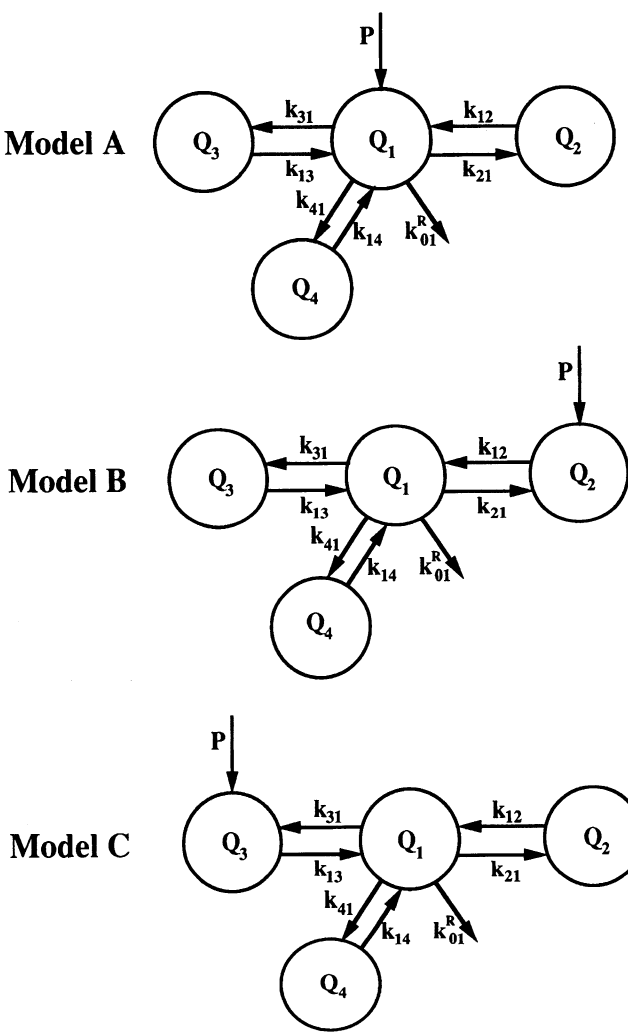

Fig. 7. Three tracee models corresponding to *model I* of Fig. 5. *Models A–C* differ in site of entry of endogenous production.

$$Q_1 = \frac{P}{k_{01}^R} \tag{22}$$

However, the situation is different for *pools 2–4*. In particular, for each of the three models, the mass of *compartment 4* cannot be estimated, whereas the tracee flux from *pool 4* to *1* ($k_{14}Q_4$) being equal to the tracee flux from *pool 1* to *4* ($k_{41}Q_1$) can be calculated. Thus the overall tracee picture we can derive will ignore the contribution of *pool 4*. For *pools 2* and *3*, it is not possible to arrive at point estimates for their mass Q_2 and Q_3. Only upper and lower bounds for Q_2 and Q_3 can be calculated

$$Q_i^{min} = Q_1 \frac{k_{i1}}{k_{1i}} \le Q_i \le Q_1 \frac{k_{i1} + k_{01}^R}{k_{1i}} = Q_i^{max} \quad i = 2, 3 \tag{23}$$

For total CO_2 in the system (Q_T), one can calculate only lower and upper values, which ignore the presence of *pool 4*; i.e., one is using only the information on Q_1, Q_2, and Q_3. One can define, as did Barstow et al. (1), Q_T^i as the total CO_2 in the system at a steady state with the assumption that all endogenous CO_2 enters the system through *pool i*

$$Q_T^1 = Q_1 + Q_2^{min} + Q_3^{min} \tag{24}$$

$$Q_T^2 = Q_1 + Q_2^{max} + Q_3^{min} \tag{25}$$

$$Q_T^3 = Q_1 + Q_2^{min} + Q_3^{max} \tag{26}$$

with

$$Q_T^{min} = Q_T^1 \le Q_T \le Q_T^3 = Q_T^{max} \tag{27}$$

Table 7 shows the bounds of the tracee masses for each subject.

DISCUSSION

Three- (1, 11, 18, 20) and two-compartment (6, 17, 21) models of bicarbonate tracer kinetics have been proposed in the literature. Our results confirm the superiority of the three- over the two-compartment model, but the novelty of the present study is the validation of a specific compartmental model structure for describing bicarbonate tracer kinetics at the whole body level. The

Table 7. *Parameter bounds for mass of tracee models of Fig. 7*

Subj No.	Q_1	Q_2^{min}	Q_2^{max}	Q_3^{min}	Q_3^{max}	Q_T^{min}	Q_T^{max}
1	2.8	2.1	2.6	8.1	13.7	13.0	18.5
2	3.1	3.5	4.3	8.2	14.2	15.0	20.7
3	4.9	2.4	3.1	9.2	14.8	16.0	22.0
4	2.2	1.4	2.0	7.2	11.0	10.7	14.5
5	3.9	6.3	8.1	4.5	10.9	14.7	21.1
6	2.7	1.7	2.1	6.4	9.2	10.8	13.5
7	2.7	1.6	2.1	7.9	12.3	12.2	16.6
8	5.3	4.8	6.3	3.8	8.6	13.9	18.6
9	3.7	3.0	4.1	4.9	9.5	11.6	16.2
Mean	3.5	3.0	3.8	6.7	11.6	13.1	18.0
±SD	±1.1	±1.6	±2.1	±1.9	±2.3	±1.9	±3.0

Values are expressed in mmol/kg.

validated structure is a mammillary three-compartment model with respiratory and nonrespiratory losses taking place in the central compartment (Fig. 5, *model I*). Whereas this model (1, 11) or a simplified two-compartment version of it obtained by lumping *pools 1* and *2* (6, 17, 21) has been proposed in the literature, it has never been validated. The open issue was not the mammillary structure or the fact that the respiratory loss takes place in the central compartment but where the nonrespiratory loss of CO_2 takes place, i.e., in the central or in one of the two peripheral compartments. By resorting to a model-structure-independent data analysis based on the body activity variable (2, 12, 16), we have been able to calculate the mean residence time in the system of particles leaving the respiratory pathway; by computing this model-independent value with that provided by the three competing tracer model structures, we have shown that the model with both irreversible losses taking place in the central compartment is the structure of choice. This finding has important implications for the execution of metabolic studies, in which the rate of oxidation of a substrate in humans is to be estimated by an isotopic method. Investigators usually infuse a carbon-labeled substrate and measure the rate of evolution of labeled CO_2 as an estimate of the rate of decarboxylation (oxidation) of the tracer. Inasmuch as a load of labeled bicarbonate, whether it is administered intravenously or intragastrically, is never entirely recovered as labeled CO_2 because of nonrespiratory losses, a correction factor needs be applied to the rate of labeled CO_2 production. This correction factor is experimentally determined by dividing the amount of labeled CO_2 recovered in the body by the labeled bicarbonate load that has been administered. The undeclared assumption underlying this approach is that the labeled bicarbonate load administered by the investigator and the labeled CO_2/HCO_3 generated by the metabolic oxidation of a substrate in the body share the same correction (recovery) factor. Although this assumption is crucial to the use of carbon-labeled tracers for the measurement of oxidative fluxes, thus far no attempts have been made to validate it. The results reported here, by demonstrating that respiratory and nonrespiratory losses are located in the central compartment, imply that the correction factor obtained by intravenous infusion of labeled bicarbonate can indeed be applied to labeled CO_2 generated by cellular metabolism of a carbon-labeled tracer and validate on theoretical and empirical grounds a procedure that has been in use for over four decades.

Another important finding concerns which measurement variable needs to be used for model identification. Very frequently the assumption is made that the CO_2 specific activity or enrichment measured in the expired air represents the central pool, where tracer input occurs (1, 6, 13, 15, 18–20). We have shown that this assumption is not appropriate, because only a fraction of the injected tracer dose is in equilibrium with the measured labeled CO_2 in the expired air. As a result, the input-output experimental configuration is not correctly described. To correct for this error, one should use a different measurement variable. We have shown that the labeled CO_2 flux in the expired air (4, 11, 17, 21) is a convenient output variable for the identification of the bicarbonate tracer model. To obtain this variable, one has to multiply the measured CO_2 specific activity or enrichment by the indirect calorimetry measurement of $\dot{V}_{CO_2}$. The $\dot{V}_{CO_2}$ information is normally available, because, as pointed out by several investigators (1, 4, 10, 11, 17, 21), it is crucial for assessing the individual respiratory and nonrespiratory losses. In this study, upper and lower values for the total body mass of HCO_3/CO_2 have been determined. The point estimates of total body mass of HCO_3/CO_2 reported in a number of previous papers were based on the unproven assumptions that production and irreversible losses of HCO_3/CO_2 take place in the central compartment. We have demonstrated that this statement is true for the HCO_3/CO_2 losses, but in agreement with Barstow et al. (1), the site(s) of HCO_3/CO_2 production remains undetermined. Thus our lower estimate for total body mass of HCO_3/CO_2 (13.2 mmol/kg body wt) is quite similar to typical textbook values [12.7 mmol/kg body wt (7)], because it assumes that HCO_3/CO_2 production is in the central compartment, whereas the upper estimate (18 mmol/kg body wt) exceeds it by $\simeq$42%. Direct measurement of the HCO_3^- concentration in the body fluids coupled with body fluid volume determinations yields an estimate of 9.2 mmol/kg body wt (7). Thus total body mass of HCO_3/CO_2 determined by tracer methods exceeds the total amount of HCO_3/CO_2 dissolved in the body fluids, thereby indicating that a significant amount of HCO_3/CO_2 in the body is present in bound form, probably in the bone. Chemical analysis of human cadavers unfortunately cannot detect the total amount of HCO_3/CO_2 with precision for technical reasons. Thus the total amount of bound HCO_3/CO_2 in the body remains undetermined: between 4 and 8.8 mmol/kg body wt.

This work was partially supported by Ministero della Universitá e della Ricerca Scientifica e Tecnologica Project "Bioingegneria dei Sistemi Metabolici e Cellulari," National Institutes of Health Grants DK-24092, DK-20579, RR-00954, and HD-20805 and General Clinical Research Center Grant M01-RR-01346, a Veterans Administration Merit Award, and funds from the Veterans Administration Medical Research Service and Geriatric Research Education and Clinical Center.

Address for reprint requests: C. Cobelli, Dept. of Electronics and Informatics, University of Padova, Via Gradenigo 6A, 35131 Padua, Italy.

Received 10 August 1993; accepted in final form 18 January 1995.

REFERENCES

1. **Barstow, T. J., D. M. Cooper, E. M. Sobel, E. M. Landaw, and S. Epstein.** Influence of increased metabolic rate on [^{13}C]bicarbonate washout kinetics. *Am. J. Physiol.* 259 (*Regulatory Integrative Comp. Physiol.* 28): R163–R171, 1990.
2. **Bergner, P. E.** Tracer dynamics and the determination of pool sizes and turnover factors in metabolic systems. *J. Theor. Biol.* 6: 137–158, 1964.
3. **Carson, E. R., C. Cobelli, and L. Finkelstein.** *The Mathematical Modeling of Metabolic and Endocrine Systems.* New York: Wiley, 1983.
4. **Cobelli, C., M. P. Saccomani, P. Tessari, G. Biolo, L. Luzi, and D. E. Matthews.** A compartmental model of leucine kinetics in humans. *Am. J. Physiol.* 261 (*Endocrinol. Metab.* 24): E539–E550, 1991.
5. **Eisenfeld, J.** On mean residence times in compartments. *Math. Biosci.* 57: 265–278, 1981.
6. **Fowle, A. S. E., C. M. E. Matthew, and E. J. M. Campbell.** The rapid distribution of $^{3}H_2O$ and $^{11}CO_2$ in the body in relation to the immediate carbon dioxide storage capacity. *Clin. Sci. Lond.* 27: 51–65, 1964.
7. **Gann, D. S., and J. F. Amaral.** Fluid and electrolyte management. In: *Essentials of Surgery*, edited by D. C. Sabiston. Philadelphia, PA: Saunders, 1987, p. 29–61.
8. **Hearon, J. Z.** Residence times in compartmental systems with and without inputs. *Math. Biosci.* 55: 247–257, 1981.
9. **Hoerr, R. A., Y.-M. Yu, D. A. Wagner, J. F. Burke, and V. R. Young.** Recovery of ^{13}C in breath from $NaNH^{13}CO_3$ infused by gut and vein: effect of feeding. *Am. J. Physiol.* 257 (*Endocrinol. Metab.* 20): E426–E438, 1989.
10. **Irving, C. S., M. R. Thomas, E. W. Malphus, L. Marks, W. W. Wong, T. W. Boutton, and P. D. Klein.** Lysine and protein metabolism in young women: subdivision based on the novel use of multiple stable isotopic labels. *J. Clin. Invest.* 77: 1321–1331, 1986.
11. **Irving, C. S., W. W. Wong, R. J. Shulman, E. O'Brian Smith, and P. D. Klein.** [^{13}C]bicarbonate kinetics in humans: intra- vs. interindividual variations. *Am. J. Physiol.* 245 (*Regulatory Integrative Comp. Physiol.* 14): R190–R202, 1983.
12. **Lassen, N. A., and W. Perl.** *Tracer Kinetic Methods in Medical Physiology.* New York: Raven, 1979.
13. **Malmendier, C. L., C. Delcroix, and M. Berman.** Interrelation in the oxidative metabolism of free fatty acids, glucose, and glycerol in normal and hyperlipemic patients. *J. Clin. Invest.* 54: 461–476, 1974.
14. **Peck, C. C., S. L. Beal, L. B. Sheiner, and A. I. Nichols.** Extended least squares nonlinear regression: a possible solution to the "choice of weights" problem in analysis of individual pharmacokinetic data. *J. Pharmacokinet. Biopharm.* 12: 545–558, 1984.
15. **Shames, D. M., M. Berman, and S. Segal.** Effects of thyroid disease on glucose oxidative metabolism in man. A compartmental model analysis. *J. Clin. Invest.* 50: 627–641, 1971.
16. **Shipley, R. A., and R. E. Clark.** *Tracer Methods for In Vivo Kinetics. Theory and Applications.* New York: Academic, 1972.
17. **Slanger, B. H., N. Kusubov, and H. S. Winchell.** Effect of exercise on human CO_2-HCO_3^- kinetics. *J. Nucl. Med.* 11: 716–718, 1970.
18. **Steele, R.** The retention of metabolic radioactive carbonate. *Biochem. J.* 60: 447–453, 1955.
19. **Umpleby, A. M., M. A. Boroujerdi, P. M. Brown, E. R. Carson, and P. H. Sonksen.** The effect of metabolic control on leucine metabolism in type 1 (insulin-dependent) diabetic patients. *Diabetologia* 29: 131–141, 1986.
20. **Waterhouse, C., N. Baker, and H. Rostami.** Effect of glucose ingestion on the metabolism of free fatty acids in human subjects. *J. Lipid Res.* 10: 487–494, 1969.
21. **Winchell, H. S., H. Stahelin, N. Kusubov, B. Slanger, M. Fish, M. Pollycove, and J. H. Lawrence.** Kinetics of CO_2-HCO_3^- in normal adult males. *J. Nucl. Med.* 11: 711–715, 1970.